POLITECNICO DI TORINO
Repository ISTITUZIONALE

# Brain Stroke Microwave Imaging via an Efficient Implementation of the CSI-FEM Algorithm

*Original*
Brain Stroke Microwave Imaging via an Efficient Implementation of the CSI-FEM Algorithm / Mariano, Valeria; Banting, Lucas; Tobon Vasquez, Jorge A.; Jeffrey, Ian; Lovetri, Joe; Vipiana, Francesca. - ELETTRONICO. - (2023). (Intervento presentato al convegno 2023 17th European Conference on Antennas and Propagation (EuCAP) tenutosi a Florence, Italy nel 26-31 March 2023) [10.23919/EuCAP57121.2023.10133102].

*Availability:*
This version is available at: 11583/2979098 since: 2023-06-05T10:54:32Z

*Publisher:*
IEEE

*Published*
DOI:10.23919/EuCAP57121.2023.10133102

*Terms of use:*

This article is made available under terms and conditions as specified in the corresponding bibliographic description in the repository

*Publisher copyright*

(Article begins on next page)

27 April 2024

# Brain Stroke Microwave Imaging via an Efficient Implementation of the CSI-FEM Algorithm

Valeria Mariano*, Lucas Banting†, Jorge A. Tobon Vasquez*, Ian Jeffrey†, Joe LoVetri† and Francesca Vipiana*
*Dept. of Electronics and Telecommunications, Politecnico di Torino, Torino, Italy, valeria_mariano@polito.it
†Dept. of Electrical and Computer Engineering, University of Manitoba, Winnipeg, Canada

***Abstract*—Microwave imaging of the human head for stroke detection is demonstrated using the finite-element contrast source inversion method with enhanced discretization of the contrast-source variable. The linear basis functions used in the new discretization lead to a simple implementation of higher accuracy compared to discretizations wherein the contrast source variable is assumed to be constant over each tetrahedron of the 3D finite-element mesh. These advantages are particularly important for stroke imaging because of the highly inhomogeneous nature of the human head. Results using synthetic data obtained from a realistic numerical model of the head show promise for stroke detection.**

***Index Terms*—brain stroke, microwave imaging, contrast source inversion method, finite element method.**

## I. Introduction

There has been an increasing interest in potential uses of Microwave imaging (MWI) in the medical field mostly because of its portability, low cost, safe use of non-ionizing radiation, and non-invasiveness. It has been applied e.g. for breast cancer diagnosis [1] and for brain stroke detection [2], [3]. The MWI working principle is the presence of a dielectric contrast between the healthy tissues and affected ones at microwave frequencies. For the solution of the resulting ill-posed inverse problem, the contrast source inversion (CSI) method can be used to quantitatively reconstruct the dielectric properties in the domain of interest (DoI) [4].

CSI is a optimization-based algorithm that minimizes a specially formed functional in the contrast and contrast-source variables. Here, the CSI algorithm works in combination with a finite element method (FEM) solver [5] that discretizes the whole volume with an unstructured and non-uniform mesh. This allows us to model the complete antenna geometry including the coaxial feed-port [6] within the synthetic environment, leading to a more realistic simulated scenario. It also allows us to include an inhomogeneous numerical background in the inversion model (similar to the procedure described in [7], [8]).

Although the field quantities use linear edge elements, FEM-CSI was originally formulated using pulse basis functions for the contrast and contrast-sources in the FEM mesh [9], [10]. Here, the aim is to present an alternative discretization, that is obtained using the basis functions of the field, also for the contrast source variable. For a simplified scenario, preliminary results are reported in [11], in which there was a comparison between the standard implementation [12] and the proposed one, through an accuracy analysis of the CSI variables discretization. Here, instead, the proposed CSI implementation is applied to reconstruct the dielectric properties of an ischemic and a hemorrhagic stroke within a 3-D multitissue head model.

The paper is organized as follows. In Sect. II there is a description of the system and the head phantom model, while Sect. III contains the description of the proposed discretization applied to the CSI method. Then, some numerical results are reported in Sect. IV and, finally, the conclusions and future developments are in Sect. V.

## II. Microwave Imaging System

In this work, the MWI system comprises an array of 24 antennas that surround the head with a helmet configuration, as depicted in Fig. 1. The antennas are low-weight and flexible and they act as both receiver and transmitter, with a working frequency of 1 GHz [6].

The MWI system is applied to a numerical 3-D anthropomorphic phantom belonging to the national library of medicine [13] and obtained via analysis of cross-sectional cryosection of a human man and a human female body, available at [14]. The phantom composition is shown in Fig. 2 with the dielectric properties (permittivity $\epsilon_r$ and conductivity $\sigma$) at 1 GHz.

Fig. 1. MWI system: antennas' array with a helmet configuration.

## III. Improved Contrast Source Inversion Method

The CSI method is an iterative algorithm that minimizes the so-called CSI cost functional. At each iteration, two variables are updated: the dielectric contrast $\chi(\underline{r})$ and the contrast source $\underline{\omega}_t(\underline{r})$. The first is the contrast between the complex

This paper's copyright is held by the author(s). It is published in these proceedings and included in any archive such as IEEE Xplore under the license granted by the "Agreement Granting EurAAP Rights Related to Publication of Scholarly Work."
Authorized licensed use limited to: Politecnico di Torino. Downloaded on June 05,2023 at 10:27:37 UTC from IEEE Xplore. Restrictions apply.

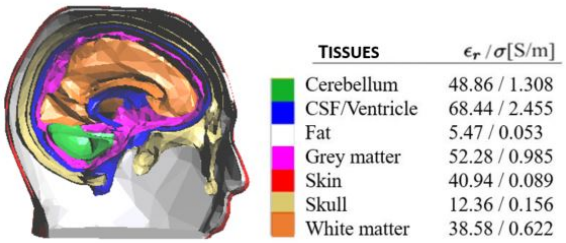


Fig. 2. Anthropomorphic 3-D head model with the permittivity $\epsilon_r$ and conductivity $\sigma$ of each tissue at 1 GHz [13].

permittivity of the background scenario $\epsilon_b(\underline{r})$ and the scenario under test $\tilde{\epsilon}(\underline{r})$, where $\underline{r}$ is the position vector in the DoI:

$$\chi(\underline{r}) \triangleq \frac{\tilde{\epsilon}(\underline{r}) - \epsilon_b(\underline{r})}{\epsilon_b(\underline{r})}. \tag{1}$$

The second variable defines equivalent sources in the DoI, that are dependent on the transmitting antenna $t$. It links the dielectric contrast $\chi(\underline{r})$ with the total field $\underline{E}_t^{\text{tot}}(\underline{r})$, when the antenna $t$ transmits:

$$\underline{\omega}_t(\underline{r}) \triangleq \chi(\underline{r})\, \underline{E}_t^{\text{tot}}(\underline{r}), \tag{2}$$

The whole volume $\Omega$ is discretized using $N$ tetrhaedral elements and the absorbing boundary conditions are imposed on the external surface of $\Omega$. The field is written as a linear combination of curl-conforming linear basis functions, $\underline{N}_e(\underline{r})$, associated with each edge $e$ of the mesh as:

$$\underline{E}_t^{\text{tot}}(\underline{r}) \cong \sum_{e=1}^{E} E_{t,e}^{\text{tot}}\, \underline{N}_e(\underline{r}) \tag{3}$$

where $E$ is the total number of edges in the mesh.

In the new discretization, the contrast-source variable and the field are written with the same vector basis, so that $\underline{\omega}_t(\underline{r})$ can be written as linear combination of a new vector basis functions:

$$\underline{\omega}_t(\underline{r}) = \sum_{n=1}^{N} \sum_{f=1}^{6} \omega_{t,(n,f)}\, \underline{\widetilde{N}}_{n,f}(\underline{r}). \tag{4}$$

where $f = 1, ..., 6$ is the local index for the edges belonging to the $n$-th tetrahedron, $\underline{\widetilde{N}}_{n,f}(\underline{r})$ is the vector basis function associated to the edge $f$ within the $n$-th tetrahedron and $\omega_{t,(n,f)}$ are scalar unknown coefficients. This basis function is, in fact, part of the basis function $\underline{N}_e(\underline{r})$: $\underline{\widetilde{N}}_{n,f}(\underline{r})$ has a domain corresponding to just one of the tetrahedra containing the considered edge. The leading benefit of this new discretization is that the update of the contrast-source variables can be applied just to the scalar coefficients $\omega_{t,(n,f)}$, preventing the use of dyadic operators, as well as vectors matrices and arrays, and making the implementation more straightforward. Moreover, the contrast-source variable keeps the same degree of variability of the discretized field, i.e. linear. Note that using this basis function, each tetrahedron can be represented as having a contrast source that is discontinuous from any of its neighbouring tetrahedra. This allows us to accurately model highly inhomogeneous regions, as in the case of the head model being considered.

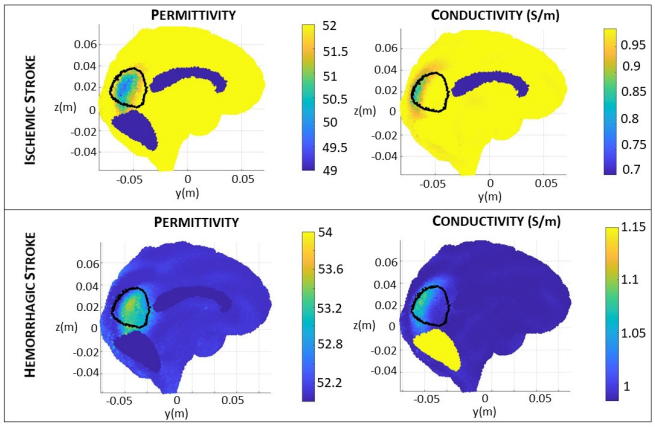


Fig. 3. CSI method results after 60 iterations. All the graphics are cut along $x = 0$ and the expected stroke perimeter is shown in black. First row: ischemic stroke, left permittivity and right conductivity. Second row: hemorrhagic stroke, left permittivity and right conductivity.

## IV. Numerical Results

The new contrast source discretization is here applied for the 3-D scenario in Fig. 2. In particular, we created two test cases with exactly the same realistic shape of the stroke, but different typology, i.e. ischemic or hemorrhagic. The analysis has been realized with a frequency equal to 1 GHz and with the following dielectric properties for the two kinds of strokes: $\epsilon_{isch} = 36.00$ and $\sigma_{isch} = 0.72\, S/m$ in the ischemic case, and $\epsilon_{hem} = 63.41$ and $\sigma_{hem} = 1.58\, S/m$ in the hemorrhagic one [15]. The whole domain is discretized through tetrahedral elements with a mesh size of the order of $\lambda/15$, considering a background medium with dielectric properties equal to the mean of all the tissue dielectric properties involved in the healthy head ($\epsilon_{mean} = 45.37$ and $\sigma_{mean} = 0.77\, S/m$). In the simulated environment, the whole antennas and the corresponding coaxial ports are completely modelled. In order to prevent the inverse crime, we use a different mesh for the generation of the scattering parameters at the antennas' ports and the computation of the incident field and the CSI method operator. The initial guess of the CSI algorithm is calculated through back-propagation [4], [16]. In Fig. 3, reconstructions of the relative permittivity and conductivity distribution after 60 iterations for the ischemic and the hemorrhagic stroke case are shown. In these figures, x=0 plane of the DoI is shown and the perimeter of the expected stroke is shown in black. The algorithm is able to identify the correct position of the stroke, especially in the permittivity distributions. Also, it correctly identifies the sign of the contrast that is negative, in the ischemic stroke, and positive, for the hemorrhagic one. In our implementation, the time needed for each iteration is around 7 minutes.

This paper's copyright is held by the author(s). It is published in these proceedings and included in any archive such as IEEE Xplore under the license granted by the "Agreement Granting EurAAP Rights Related to Publication of Scholarly Work."
Authorized licensed use limited to: Politecnico di Torino. Downloaded on June 05,2023 at 10:27:37 UTC from IEEE Xplore. Restrictions apply.

## V. Conclusion and Perspectives

In this paper, an alternative method to discretize the contrast source variable has been presented. It allows develop the complete CSI method procedure using scalar quantities, leading to a straightforward implementation. We have reported the performances of the proposed algorithm in a realistic 3-D scenario in a multitissue head phantom. The two test cases have the same shape and position of the stroke, but different typology (ischemic and hemorrhagic). The results have shown that the algorithm is able to identify the stroke location in both the tests and also the sign of the dielectric contrast inside the stroke.

Future development deals with the use of the developed imaging algorithm with measured data obtained via the MWI system in [3] applied to a multi-tissue head phantom. Extra results, such as the comparison between the performance obtained through the new discretization and the standard one, will be presented in the conference.

## Acknowledgment

This work was supported in part by the European Union's Horizon 2020 research and innovation program under the EMERALD project, Marie Skłodowska-Curie grant agreement No. 764479 and in part by the project PON Research and Innovation "Microwave Imaging and Detection powered by Artificial Intelligence for Medical and Industrial Applications (DM 1062/21)," funded by the Italian Ministry of University and Research (MUR)

## References

[1] T. M. Grzegorczyk, P. M. Meaney, P. A. Kaufman, R. M. diFlorio Alexander, and K. D. Paulsen, "Fast 3-d tomographic microwave imaging for breast cancer detection," *IEEE Transactions on Medical Imaging*, vol. 31, no. 8, pp. 1584–1592, 2012.

[2] A. Fhager, S. Candefjord, M. Elam, and M. Persson, "Microwave diagnostics ahead: Saving time and the lives of trauma and stroke patients," *IEEE Microwave Magazine*, vol. 19, no. 3, pp. 78–90, 2018.

[3] J. A. Tobon Vasquez, R. Scapaticci, G. Turvani, G. Bellizzi, D. O. Rodriguez-Duarte, N. Joachimowicz, B. Duchêne, E. Tedeschi, M. R. Casu, L. Crocco, and F. Vipiana, "A prototype microwave system for 3D brain stroke imaging," *Sensors*, vol. 20, May 2020.

[4] A. Zakaria, C. Gilmore, and J. LoVetri, "Finite-element contrast source inversion method for microwave imaging," *Inverse Problems*, vol. 26, pp. 115 010–21, 11 2010.

[5] D. O. Rodriguez-Duarte, J. A. Tobon Vasquez, R. Scapaticci, L. Crocco, and F. Vipiana, "Assessing a microwave imaging system for brain stroke monitoring via high fidelity numerical modelling," *IEEE J. Electromagn., RF, Microw. Med. Biol.*, vol. 5, no. 3, pp. 238–245, Sept. 2021.

[6] D. O. Rodriguez-Duarte, C. Origlia, J. A. T. Vasquez, R. Scapaticci, L. Crocco, and F. Vipiana, "Experimental assessment of real-time brain stroke monitoring via a microwave imaging scanner," *IEEE Open Journal of Antennas and Propagation*, vol. 3, pp. 824–835, July 2022.

[7] D. Kurrant, A. Baran, J. LoVetri, and E. Fear, "Integrating prior information into microwave tomography part 1: Impact of detail on image quality," *Medical Physics*, vol. 44, pp. 6461–81, 09 2017.

[8] ——, "Integrating prior information into microwave tomography part 2: Impact of errors in prior information on microwave tomography image quality," *Medical Physics*, vol. 44, pp. 6482–503, 09 2017.

[9] A. Zakaria and J. LoVetri, "The finite-element method contrast source inversion algorithm for 2d transverse electric vectorial problems," *IEEE Transactions on Antennas and Propagation*, vol. 60, no. 10, pp. 4757–4765, 2012.

[10] A. Zakaria, I. Jeffrey, and J. LoVetri, "Full-vectorial parallel finite-element contrast source inversion method," *Progress in Electromagnetics Research-pier*, vol. 142, pp. 463–483, 2013.

[11] V. Mariano, J. A. Tobon Vasquez, and F. Vipiana, "Discretization error analysis in the contrast source inversion algorithm," in *2021 15th European Conference on Antennas and Propagation (EuCAP)*, 2021, pp. 1–4.

[12] A. Zakaria, "The finite-element contrast source inversion method for microwave imaging applications," Ph.D. dissertation, Univ. of Manitoba, 2012.

[13] S. N. Makarov, G. M. Noetscher, J. Yanamadala, M. W. Piazza, S. Louie, A. Prokop, A. Nazarian, and A. Nummenmaa, "Virtual human models for electromagnetic studies and their applications," *IEEE Reviews in Biomedical Engineering*, vol. 10, pp. 95–121, 2017.

[14] D.Andreuccetti, R.Fossi, and C.Petrucci. Download visible human project data. [Online]. Available: https://www.nlm.nih.gov/databases/download/vhp.html

[15] ——. An internet resource for the calculation of the dielectric properties of body tissues in the frequency range 10 hz - 100 ghz. ifac-cnr, florence (italy), 1997. based on data published by c.gabriel et al. in 1996. [Online]. Available: http://niremf.ifac.cnr.it/tissprop/

[16] P. M. van den Berg and A. Abubakar, "Contrast source inversion method: State of art," in *Progress In Electromagnetics Research*, vol. 34, 2001, pp. 189–218.

This paper's copyright is held by the author(s). It is published in these proceedings and included in any archive such as IEEE Xplore under the license granted by the "Agreement Granting EurAAP Rights Related to Publication of Scholarly Work."
Authorized licensed use limited to: Politecnico di Torino. Downloaded on June 05,2023 at 10:27:37 UTC from IEEE Xplore. Restrictions apply.